Twin boundary profiles with linear-quadratic coupling between order parameters

2014 J. Phys.: Condens. Matter 26 342201

(http://iopscience.iop.org/0953-8984/26/34/342201)

OPEN ACCESS
IOP Publishing

Fast Track Communications
Journal of Physics: Condensed Matter

J. Phys.: Condens. Matter **26** (2014) 342201 (6pp) doi:10.1088/0953-8984/26/34/342201

Fast Track Communication

Twin boundary profiles with linear-quadratic coupling between order parameters

Henning Pöttker[1] **and Ekhard K H Salje**[2]

[1] Institut für Angewandte Mathematik, Universität Bonn, Endenicher Allee 60, 53115 Bonn, Germany
[2] Department of Earth Sciences, University of Cambridge, Downing Street, Cambridge CB2 3EQ, UK

E-mail: poettker@iam.uni-bonn.de and ekhard@esc.cam.ac.uk

Received 27 May 2014, revised 24 June 2014
Accepted for publication 3 July 2014
Published 28 July 2014

Abstract

A new type of twin boundary was found when two order parameters interact by linear-quadratic coupling QP^2. In this solution, we find that a domain wall consists of two layers in which in one layer both order parameters Q and P are active while in the second layer only Q is active. The adjacent domains are equally asymmetric (Q, P) and $(Q, 0)$ so that one phase could be polar and/or magnetic and contain a ferroelastic strain while the second layer is ferroelastic only without polar or magnetic properties. The two layers represent a stepwise transition between the two domains.

We analyze the full phase diagram depending on the coupling constant and anisotropy of the gradient term, and show that in a certain regime the order parameter Q becomes activated only in the interfacial region. A common solution contains kinks and breathers whereby the width of the interface can be very wide in agreement with the first order character of the transition.

Keywords: domain boundaries, order parameter coupling, twin wall, multiferroic, Landau Ginzburg theory, microstructure

(Some figures may appear in colour only in the online journal)

1. Introdcution

A major progress in solid state science is the understanding that interfaces are not (always) just the 'zip' between adjacent domain structures which have no properties and cannot be found in the bulk of the domains. Until 1955, the idea of twins as 'zips' between domains dominated, then more advanced theories, such as Landau Ginzburg theory became popular and the trajectories were calculated including the minimization of the local strain energy and surface tension [1–6].

Today, the emphasis lies on the question: can we modify interfaces in such a way that they display novel properties which have nothing to do with the properties we find in the bulk of the domains. The idea that such properties exist is new [4, 6]. 'Exotic' interfaces were previously either rejected as wrong observations or taken as exceptions to the 'normal' behaviour, which could be safely ignored. The fact that we can generate interfaces such as twin boundaries in an engineering fashion, which are good conductors in an insulating matrix [7–10], or ferroelectric interfaces when the matrix is non-polar [11–15], or when magnetic interfaces are expected in non-magnetic materials [16–18], adds emphasis to the field of Domain Boundary Engineering [6], which has as its goal, to produce interfaces which have properties that do not exist in the bulk and which are useful as memory devices and other device applications. There are only a few confirmed materials where the domain boundary engineering has succeeded: WO_3 (superconducting walls [8]), $BiFeO_3$ and $LiNbO_3$ (conducting walls [9, 19]), $SrTiO_3$, and $CaTiO_3$ (polar walls [12–15]) are certainly amongst them.

The most successful approach to develop a proper theory of domain boundary engineering uses the following concept: we know that phase diagrams depend sensitively on the competition of various phases whereby a stable phase is determined

by its absolute minimum of some energy functional such as the Gibbs free energy. For infinite solids the construction of such energies is well understood within the framework of Landau theory. Modifications are needed for boundary conditions and are also generally understood for most relevant geometrical scenarios. The problem becomes more complicated when interfaces are considered because the energy minimization needs to be done under the appropriate boundary conditions and surface terms need to be added explicitly to describe the fact that we want to know what phases exist in the quasi-two dimensional lattice of the interface. Polar twin boundaries in $CaTiO_3$ are a typical example. No polar phases exist in $CaTiO_3$ but polarity is a physical property closely related to the structure type of $CaTiO_3$. The approach is then to assume that an unstable (or metastable) phase with a well-defined polarity interacts with the structural state of the stable state. If we define each state by their thermodynamic order parameter (e.g. Q for the stable deformation and P for the polarity) then we can formulate the Gibbs free energy as an energy including a coupling term between deformation and polarity of the kind $Q^n P^m$ where the order of the coupling is given by the exponents n and m. The parameters n and m are determined by symmetry, in our example $n = m = 2$ for $CaTiO_3$.

The case of bi-linear coupling $n = m = 1$ is rare but well documented for the bulk [20, 21]. The bi-quadratic coupling $n = m = 2$ is the most common and was first identified by Houchmanzadeh *et al* [5], and explored in detail by Conti *et al* [22]. The case of linear-quadratic coupling ($n = 1, m = 2$) is new and has been first analyzed as a new type of interaction by Salje and Carpenter [23]. Here we explore the consequences of such coupling for interfacial properties where Q forms a twin boundary and P reacts to these boundary conditions. The paper is organized as follows: we formulate the Gibbs free energy in part 2, we then discuss the solutions in part 3 and compare the results with possible applications in part 4.

2. The model

2.1. The Gibbs free energy and the interfacial energy

As in [23], we write the Gibbs free energy as

$$G_{a,c,\lambda}(Q, P) = \frac{1}{2}aQ^2+\frac{1}{4}Q^4+\frac{1}{2}cP^2+\frac{1}{4}P^4+\frac{1}{2}\lambda QP^2+g_{a,c,\lambda}$$

where $a, c, \lambda \in \mathbb{R}, \lambda \neq 0$ and a normalization constant $g_{a,c,\lambda} \geqslant 0$ is added such that the minimum of $G_{a,c,\lambda}$ is zero. Taking the leading-order gradient term for each order parameter into account, the total energy of an interface is

$$E_{a,c,\lambda,\kappa_1,\kappa_2}[u, v] = \int_{\mathbb{R}} G_{a,c,\lambda}(u, v)+\kappa_1 \left|u'\right|^2+\kappa_2 \left|v'\right|^2 \,\mathrm{d}x \quad (1)$$

where $\kappa_1, \kappa_2 > 0$ and $u, v : \mathbb{R} \to \mathbb{R}$ represent Q and P, respectively. This energy has to be minimized over all pairs (u, v) that attain stable points of the Gibbs free energy as $x \to \pm\infty$. The rescalings

$$\tilde{u}(x) = \mu u(\nu x)$$
$$\tilde{v}(x) = \mu v(\nu x)$$

with $\mu \in \mathbb{R}$ and $\nu > 0$ together with the identities

$$\mu^4 G_{a,c,\lambda}(Q, P) = G_{\mu^2 a,\mu^2 c,\mu\lambda}(\mu Q, \mu P),$$
$$\frac{\mu^4}{\nu} E_{a,c,\lambda,\kappa_1,\kappa_2}[u, v] = E_{\mu^2 a,\mu^2 c,\mu\lambda,(\mu/\nu)^2\kappa_1,(\mu/\nu)^2\kappa_2}[\tilde{u}, \tilde{v}]$$

allow to fix the coupling constant $\lambda = -1$ and to consider only the relative strength of the gradient terms $\kappa = \kappa_2/\kappa_1 > 0$. It remains to consider the energy

$$E_{a,c,\kappa} = \int_{\mathbb{R}} G_{a,c,-1}(u, v) + \left|u'\right|^2 + \kappa \left|v'\right|^2 \,\mathrm{d}x.$$

For conciseness, we will hereafter write $G = G_{a,c,\lambda}$ and $E = E_{a,c,\kappa}$ when the notation is unambiguous.

2.2. The stable points of the Gibbs free energy

The interfaces link stable points of G. Thus, the first step in characterizing all possible profiles is a precise characterization of the stable points and their dependence on a and c. Inspection of $G = G_{a,c,-1}$ yields that if (Q, P) is one of its stable points, then

- also $(Q, -P)$ is stable,
- if in addition $P = 0$, then also $(-Q, 0)$ is stable,
- if in addition $P \neq 0$, then $Q \geqslant 0$.

Possible minimizers of G are its critical points, i.e. real solutions of

$$0 = \partial G/\partial Q = Q^3 + aQ - \frac{1}{2}P^2,$$
$$0 = \partial G/\partial P = P\left(P^2 + c - Q\right).$$

These are $(0, 0)$, $\left(\pm\sqrt{-a}, 0\right)$ if $a \leqslant 0$, and real solutions of

$$0 = Q^3 + \left(a - \frac{1}{2}\right)Q + \frac{1}{2}c, \qquad P^2 = -c + Q. \quad (2)$$

If real solutions (Q, P) of (2) exist, the largest such Q shall be denoted as $Q_0 = Q_0(a, c)$ and the corresponding non-negative P as $P_0 = P_0(a, c)$.

A careful analysis yields that the sets of actual minimizers of G fall into three categories that divide the a-c-plane into three subsets as visualized in figure 1:

$$A_1 = \left\{0 \leqslant a \leqslant \frac{1}{2}, \gamma(a) \leqslant c\right\} \cup \left\{\frac{1}{2} \leqslant a, 0 \leqslant c\right\},$$
$$A_2 = \left\{a \leqslant -\frac{1}{4}, \sqrt{-a} \leqslant c\right\} \cup \left\{-\frac{1}{4} \leqslant a \leqslant 0, \frac{1}{4} - a \leqslant c\right\},$$
$$A_3 = \mathbb{R}^2 \setminus (A_1 \cup A_2).$$

where $\gamma : [0, 1/2] \to [0, 1/4]$ is implicitly defined by

$$0 = G\left(Q_0(a, \gamma(a)), P_0(a, \gamma(a))\right).$$

Then:

(i) If $(a, c) \in A_1$, then $(Q, P) = (0, 0)$ is stable.
(ii) If $(a, c) \in A_2$, then $(Q, P) = \left(\pm\sqrt{-a}, 0\right)$ are stable.
(iii) If $(a, c) \in A_3$, then $(Q, P) = (Q_0, \pm P_0)$ are stable.

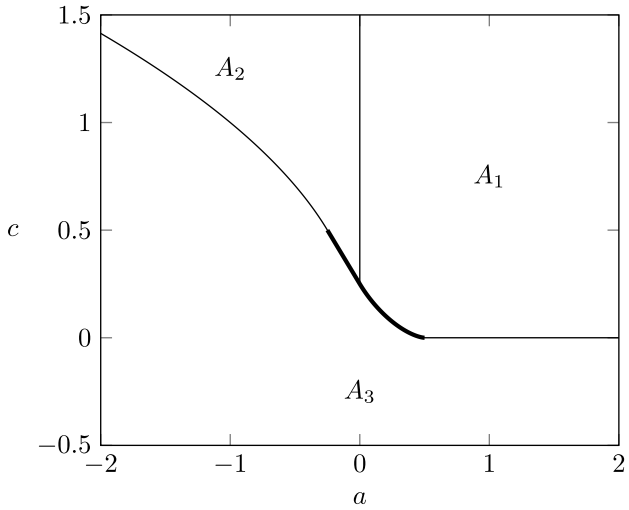

Figure 1. Partition of the a-c-plane into the sets A_1, A_2 and A_3. Minimizers of G are only discontinuous across the thick part of the borders.

Furthermore, in the interior of each set the stable points enumerated above are the only stable points. Within each set the stable points depend continuously on a and c. However:

- For $(a, c) \in A_1 \cap A_2$ the stable points of (i) and (ii) coincide.
- For $(a, c) \in A_1 \cap A_3$ the stable points of (i) and (iii) coincide if and only if $1/2 \leqslant a$.
- For $(a, c) \in A_2 \cap A_3$ the stable points of (ii) and (iii) coincide if and only if $a \leqslant -1/4$.

3. Results

We now discuss different interfaces that arise depending on whether the parameters (a, c) lie in the sets A_1, A_2, A_3 or their pairwise intersections. The findings are illustrated by results of finite-element simulations.

3.1. $(a, c) \in A_1$ *such that only* $(0, 0)$ *is stable*

In this case, interfaces can only link the state $(0, 0)$ with itself and E is minimized over all pairs $(u, v) : \mathbb{R} \to \mathbb{R}^2$ such that $(u, v)(\pm\infty) = (0, 0)$. Trivially, the unique minimizers are constantly zero.

3.2. $(a, c) \in A_2$ *and* $a < 0$ *such that only* $(\pm\sqrt{-a}, 0)$ *are stable*

Up to symmetry, all (non-constant) interfaces are in the admissible set

$$\mathcal{A} = \left\{ (u, v) : \mathbb{R} \to \mathbb{R}^2 \;\middle|\; (u, v)(\pm\infty) = (\pm\sqrt{-a}, 0) \right\}.$$

First consider the limiting case $\kappa = 0$. Then

$$\min_{\mathcal{A}} \int_{\mathbb{R}} G(u, v) + \left|u'\right|^2 \mathrm{d}x = \min_{\mathcal{A}_0} \int_{\mathbb{R}} \min_{P} G(u, P) + \left|u'\right|^2 \mathrm{d}x$$

where

$$\mathcal{A}_0 = \left\{ u : \mathbb{R} \to \mathbb{R} \mid u(\pm\infty) = \pm\sqrt{-a} \right\}.$$

A straightforward computation yields

$$\arg\min_{P} G(Q, P) = \begin{cases} 0, & \text{for } Q \leqslant c, \\ \pm\sqrt{Q - c}, & \text{for } Q > c. \end{cases} \tag{3}$$

Since $(a, c) \in A_2$ implies $\sqrt{-a} \leqslant c$, the minimization problem left to solve is

$$\min_{\mathcal{A}} \int_{\mathbb{R}} G(u, v) + \left|u'\right|^2 \mathrm{d}x = \min_{\mathcal{A}} \int_{\mathbb{R}} \frac{1}{2}au^2 + \frac{1}{4}u^4 + \left|u'\right|^2 \mathrm{d}x$$

which has the well-known solutions

$$u(x) = \sqrt{-a}\tanh\left(\frac{1}{2}\sqrt{-a}\,(x - x_0)\right), \qquad x_0 \in \mathbb{R}. \tag{4}$$

By (3) the corresponding v is constantly zero. The minimizers for $\kappa > 0$ are exactly the same pairs (u, v) since if there existed a pair $(\tilde{u}, \tilde{v})$ with $E_{a,c,\kappa}[\tilde{u}, \tilde{v}] < E_{a,c,\kappa}[u, v]$ then $v = 0$ would imply

$$E_{a,c,0}[\tilde{u}, 0] \leqslant E_{a,c,\kappa}[\tilde{u}, \tilde{v}] < E_{a,c,\kappa}[u, v] = E_{a,c,0}[u, 0].$$

The interfaces are plotted in figure 2.

3.3. $(a, c) \in A_3$ *such that only* $(Q_0, \pm P_0)$ *are stable*

In this case, all interfaces up to symmetry lie in

$$\mathcal{A} = \left\{ (u, v) : \mathbb{R} \to \mathbb{R}^2 \;\middle|\; (u, v)(\pm\infty) = (Q_0, \pm P_0) \right\}. \tag{5}$$

In contrast to the previous case, we are not aware of the existence of closed expressions for the minimizers. However, they can be computed numerically and two typical profiles are plotted in figure 3.

For all $\kappa > 0$ the length scale of the transition is of order $\sqrt{\kappa}$. If $\kappa << 1$ 'jumps' of v are only weakly penalized and v changes quickly while u remains roughly constant. As $\kappa \to \infty$ the maximal distance of u from its boundary value Q_0 increases and its minimal value approaches $\sqrt{\max\{-a, 0\}}$ continuously. In the limiting case $\kappa = \infty$, which can be realized by setting $\kappa_1 = 0$ in the original formulation (1) of E, the interface passes through the point $(\sqrt{\max\{-a, 0\}}, 0)$. This can be confirmed by an explicit calculation along the lines of the previous subsection.

3.4. $(a, c) \in A_1 \cap A_3$ *such that* $(0, 0)$ *and* $(Q_0, \pm P_0)$ *are stable*

As in subsection 3.3., we consider interfaces that link the states $(Q_0, \pm P_0)$, i.e. profiles in the set $\mathcal{A}$ given in (5). For small κ, the picture is similar and the interfaces are well separated from the now stable point $(0, 0)$.

However, for fixed a and c there exists a critical value κ^* such that for $\kappa > \kappa^*$, the point $(0, 0)$ gets activated and the interface is divided into two separate transitions between

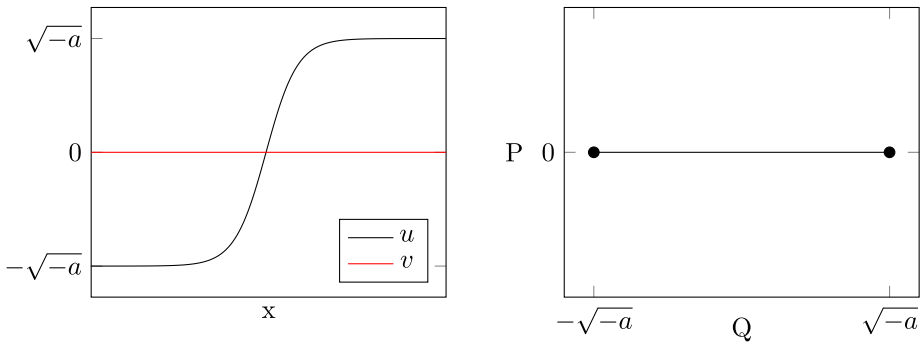

Figure 2. Optimal interfaces as functions of x (left) and in the (Q, P)-plane (right) for $(a, c) \in A_2$ as in subsection 3.2. and $\kappa \geqslant 0$. Because $v = 0$, the curves are independent of κ. The dots mark the stable states of G.

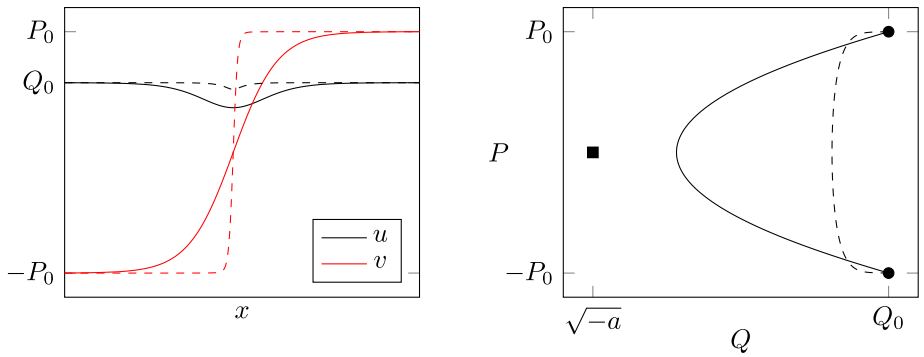

Figure 3. Optimal interfaces as functions of x (left) and in the (Q, P)-plane (right) for $(a, c) \in A_3$ as in subsection 3.3. with two distinct stable states $(Q_0, \pm P_0)$. The parameters are $a = -1$, $c = -10$, $\kappa = 10$ (full) and $\kappa = 0.1$ (dashed). The dots mark the stable states. The square marks the unstable point $(\sqrt{-a}, 0)$ which the profiles approach steadily as $\kappa \to \infty$.

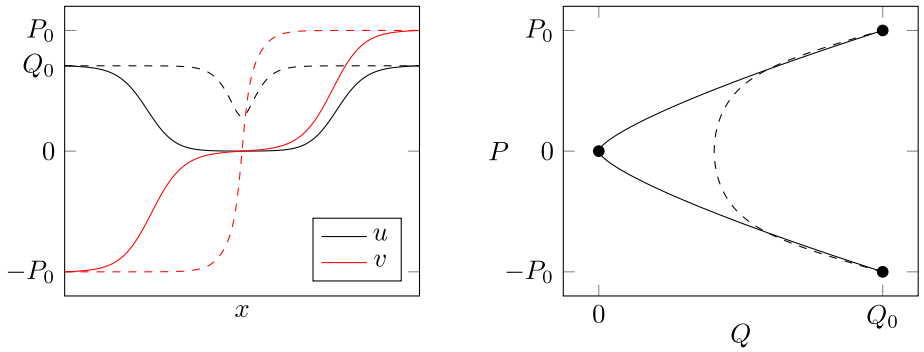

Figure 4. Optimal interfaces as functions of x (left) and in the (Q, P)-plane (right) for $(a, c) \in A_1 \cap A_3$ as in subsection 3.4. with three distinct stable states $(0, 0)$ and $(Q_0, \pm P_0)$. The chosen parameters are $a = 0.24$, $c = 0.08$, $\kappa = 1$ (full) and $\kappa = 0.1$ (dashed). For large κ, the stable point $(0, 0)$ gets activated. The dots mark the stable states.

$(Q_0, -P_0)$ and $(0, 0)$ and between $(0, 0)$ and (Q_0, P_0). With the class of partial interfaces

$$\mathcal{A}' = \{(u, v) \mid (u, v)(-\infty) = (0, 0), (u, v)(\infty) = (Q_0, P_0)\}$$

κ^* can be characterized implicitly by the equality

$$\min_{\mathcal{A}} E_{a,c,\kappa*} = 2 \min_{\mathcal{A}'} E_{a,c,\kappa*}.$$

We are unaware of a general explicit characterization. Figure 4 visualizes the dichotomy for $a = 0.24$ and $c = 0.08$ where $0.1 < \kappa^* < 1$.

The phenomenon can roughly be explained as follows. The Gibbs free energy G consists of a 2-4-potential for each of the order parameters Q and P and the coupling term $\lambda Q P^2$. The closer the order parameters (Q, P) pass the point $(0, 0)$ the weaker the coupling term gets. If they are close enough, the uncoupled potentials dominate and Q and P seek their stable points which is 0 for both, since $a, c \geqslant 0$.

3.5. $(a, c) \in A_2 \cap A_3$ such that $(\pm\sqrt{-a}, 0)$ and $(Q_0, \pm P_0)$ are stable

The interfaces displaying new features not covered in previous subsections lie in

$$\mathcal{A} = \big\{(u, v) \,\big|\, (u, v)(-\infty) = (-\sqrt{-a}, 0), \quad (u, v)(\infty) = (Q_0, P_0)\big\}.$$

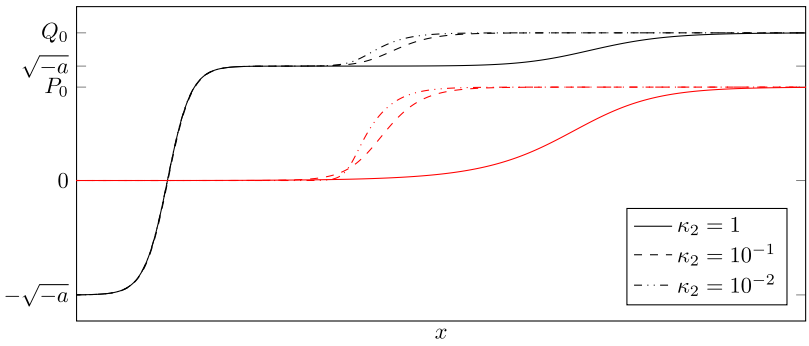

Figure 5. Optimal interfaces as functions of x for $(a, c) \in A_2 \cap A_3$ as in subsection 3.5. with four distinct stable states $(\pm\sqrt{-a}, 0)$ and $(Q_0, \pm P_0)$. The chosen parameters are $a = -0.15$, $c = 0.4$, $\lambda = -1$, $\kappa_1 = 1$ and κ_2 is indicated by the line type. The black curves represent u, the red/grey curves represent v. The two transitions are well-separated and have a common length scale for $\kappa = \kappa_2/\kappa_1 << 1$.

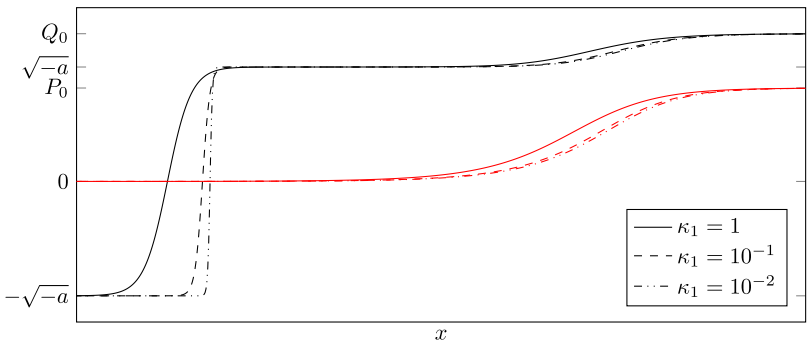

Figure 6. Optimal interfaces as in figure 5 but with $\kappa_2 = 1$ fixed and κ_1 indicated by the line type. The two transitions are well-separated. While the length scale of the second transition is constant the length scale of the first shrinks like $\sqrt{1/\kappa} = \sqrt{\kappa_1/\kappa_2}$ as $\kappa \to \infty$.

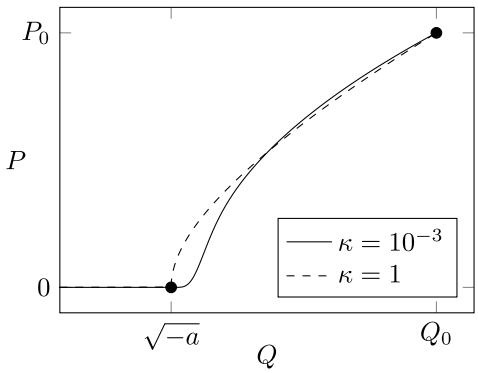

Figure 7. Optimal interfaces of figures 5 and 6 in the (Q, P)-plane. The value of κ is indicated by the line type.

Numerical evidence and the rigorous results of subsection 3.2. suggest that optimal interfaces in this class split for all $\kappa > 0$ into a transition joining the pure phases $(\mp\sqrt{-a}, 0)$ and another joining $(\sqrt{-a}, 0)$ with (Q_0, P_0). Interfaces for several values of κ are plotted in figures 5 and 6 as functions of x and in figure 7 in the Q-P-plane.

In the first transition, the order parameter v is suppressed and remains zero while u takes the form (4) as in subsection 3.2.. The first transition region has constant length and is independent of κ. In terms of the original coefficients κ_1 and κ_2 from (1), it is of order $\sqrt{\kappa_1}$ and in particular, is independent of κ_2.

The second transition is well separated from the first and the partial interface joins different values for both u and v, respectively. Hence, its length scale is determined by the stronger gradient term, i.e. of order $\max\{\sqrt{\kappa_1}, \sqrt{\kappa_2}\}$ or $\max\{1, \sqrt{\kappa}\}$ in terms of κ.

The reason why the interfaces always split is roughly as follows. During the first transition, the coupling term is dominated by the uncoupled potentials whose stable points are $\pm\sqrt{-a}$ for u and 0 for v since here $a < 0$ and $c > 0$. It is only during the second transition that the values of u are large enough to activate the coupling term.

4. Discussion

The various wall profiles contain simple twin walls with only one active order parameter whereby the second order parameter is uniformly depressed in the wall and in the bulk (figure 2). The second classic solution are kinks and breathers where P changes sign and Q changes only in the domain wall (figures 3 and 4). This solution is not chiral because Q reduces from an equilibrium value Q_0, the equivalent enhancement from Q_0 is not possible and hence there is no chiral order in this configuration, in contrast to the results from bi-quadratic coupling [22]. The novel solution in figures 5 and 6 show double kinks which are exciting when u goes from $-$ to $+$ while v remains non-negative. This constitutes double walls: in part of the wall the changes are mainly in v, then u changes. This constitutes two layers which are stuck together. Their

stability stems from the two adjacent domains where in one domain Q and P are active while the second domain has only Q but not P as an active component. Hence, the transition between these two domains is stepwise with Q and P reacting differently in different parts of the wall.

The new type of walls have been found mathematically but not experimentally. Where can we expect them to exist? Several options can be imagined:

1. If the volume strain is large (such as quartz SiO_2), one could imagine a Dauphine wall to have a second 'volume' wall next to it. That would have consequences for the description of the incommensurate phase [24–26]. The usual rigid unit calculations do not consider this effect and hence may be wrong [27].
   It also means that walls have an asymmetry with the $v = 0$ state on one side but not the other. Walls would then have a 'direction' which again stems from the broken symmetry. In incommensurate phases, such directions have never been considered.
   In a milder way, $BaTiO_3$ has a volume anomaly which goes with a dipole moment as driving order parameter. Does this mean that 180° walls (in P) have a volume component next to it? So far the evidence is against this, i.e. the walls are very thin. The usual theory does not consider volume. This is different for 90° walls where strain effects are important and the shape of the walls may be asymmetric [28, 29].
2. Magnetic systems are Fe–O (wuestite) and MnO near the Vervey transition [16]. Here, the experimental resolution is poor. The damping of wall movements is very well measured, however, and we may be able to extract data from there.
3. In a wider context, it is possible that walls with asymmetric charge distributions fall into the same set of problems. If charges appear on one side of the wall but not on the other, then they follow the same profiles as discussed in this paper. Such scenarios were discussed by Eliseev *et al* [30]. Similarly, the interfaces between SrTiO and $LaAlO_3$ may contain topological defects which also generate asymmetric wall profiles [31]. Effects of linear-quadratic order parameter coupling are indeed expected in these cases.

Other asymmetric walls may arise from the flexoelectric effect at the walls that lead to Neel-like polarization components at the otherwise Ising-like walls [32] where asymmetries may occur so that one needs to take our current results into account if the order parameter coupling is formulated.

Acknowledgments

The authors thank S Müller for fruitful discussions on the subject of the paper. HP is supported by the German Research Foundation (DFG) via SFB 1060 - *The Mathematics of Emergent Effects*. EKHS thanks the Leverhulme foundation (RG66640) and EPSRC (RG66344) for financial support.

References

[1] Hayward S A *et al* 1996 *Eur. J. Miner.* **8** 1301–10
[2] Ball J M and Crooks E C M 2011 *Calcul. Variations PDE* **40** 501–38
[3] Stepkova V, Marton P and Hlinka J 2012 *J. Phys.: Condens. Matter* **24** 212201
[4] Salje E and Zhang H 2009 *Phase Trans.* **82** 452–69
[5] Houchmandzadeh B, Lajzerowicz J and Salje E 1991 *J. Phys.: Condens. Matter* **3** 5163–9
[6] Salje E K H 2010 *ChemPhysChem* **11** 940–50
[7] Seidel J *et al* 2010 *Phys. Rev. Lett.* **105** 197603
[8] Kim Y, Alexe M and Salje E K H 2010 *Appl. Phys. Lett.* **96** 032904
[9] Maksymovych P *et al* 2011 *Nano Lett.* **11** 1906–12
[10] Chiu Y *et al* 2011 *Adv. Mater.* **23** 1530–4
[11] Salje E K H *et al* 2013 *Phys. Rev. Lett.* **111** 247603
[12] Van Aert S *et al* 2012 *Adv. Mater.* **24** 523
[13] Goncalves-Ferreira L *et al* 2008 *Phys. Rev. Lett.* **101** 097602
[14] Goncalves-Ferreira L *et al* 2010 *Phys. Rev.* B **81** 024109
[15] Zykova-Timan T and Salje E K H 2014 *Appl. Phys. Lett.* **104** 082907
[16] Zhang Z *et al* 2012 *J. Phys.: Condens. Matter* **24** 215404
[17] Brok E *et al* 2014 *Phys. Rev.* B **89** 054430
[18] Oravova L *et al* 2013 *J. Phys.: Condens. Matter* **25** 259501
[19] Schröder M, Haußmann A, Thiessen A, Soergel E, Woike T and Eng L M 2012 *Adv. Funct. Mater.* **22** 3936–44
[20] Camara F, Doukhan J C and Salje E K H 2000 *Phase Trans.* **71** 227–42
[21] Salje E 1985 *Phys. Chem. Miner.* **12** 93–8
[22] Conti S, Müller S, Poliakovsky A and Salje E K H 2011 *J. Phys.: Condens. Matter* **23** 142203
[23] Salje E K H and Carpenter M A 2011 *J. Phys.: Condens. Matter* **23** 462202
[24] Aslanian T A and Levanyuk A P 1979 *Solid State Commun.* **31** 547–50
[25] Dmitriev S V *et al* 1997 *Phys. Rev.* B **55** 8155–64
[26] Carpenter M A *et al* 1998 *Am. Miner.* **83** 2–22
[27] Hammonds K D *et al* 1996 *Am. Miner.* **81** 1057–79
[28] Ishibashi Y and Salje E 2002 *J. Phys. Soc. Japan* **71** 2800–3
[29] Ishibashi Y, Iwata M and Salje E 2005 *Japan. J. Appl. Phys. Part 1: Regul. Pap. Brief Commun. Rev. Pap.* **44** 7512–7
[30] Eliseev E A, Morozovska A N, Svechnikov G S, Gopalan V and Shur V Y 2001 *Phys. Rev.* B **83** 235313
[31] Salje E K H and Carpenter M A 2011 *Appl. Phys. Lett.* **99** 051907
[32] Gu Y, Li M, Morozovska A N, Wang Y, Eliseev E A, Gopalan V and Chen L-Q 2014 *Phys. Rev.* B **89** 174111